Ellipticine derivative NSC 338258 represents a potential new antineoplastic agent for the treatment of multiple myeloma

Erming Tian,[1] Terry H. Landowski,[2] Owen W. Stephens,[1] Shmuel Yaccoby,[1] Bart Barlogie,[1] and John D. Shaughnessy, Jr.[1]

[1]The Donna D. and Donald M. Lambert Laboratory of Myeloma Genetics, Myeloma Institute for Research and Therapy, University of Arkansas for Medical Sciences, Little Rock, Arkansas and [2]Department of Medicine, Arizona Cancer Center, University of Arizona, Tucson, Arizona

Abstract

High-risk multiple myeloma can be correlated with amplification and overexpression of the cell cycle regulator *CKS1B*. Herein, we used the COMPARE algorithm to correlate high expression of *CKS1B* mRNA in the NCI-60 cell line panel with the concentration causing 50% growth inhibition (GI_{50}) of >40,000 synthetic compounds. This led to the identification of NSC 338258 (EPED3), a highly stable, hydrophilic derivative of the plant alkaloid ellipticine. *In vitro*, this synthetic anticancer compound exhibits dramatic cytotoxic activity against myeloma cells grown in suspension or in coculture with stromal cells. EPED3-induced cell cycle arrest and an apoptotic progression that appear to be a consequence of the instantaneous effect of the drug on cytoplasmic organelles, particularly mitochondria. Disruption of mitochondria and cytoplasmic distribution of cytochrome *c* initiated the intracellular proteolytic cascade through the intrinsic apoptotic pathway. EPED3 is able to induce apoptosis in myeloma cells with *de novo* or acquired resistance to commonly administered anti-myeloma agents. Collectively, our data suggest that EPED3 targets mitochondrial function to rapidly deplete chemical energy and initiate apoptosis in myeloma cells at nanomolar concentrations while leaving stromal cells unharmed. [Mol Cancer Ther 2008;7(3):500–9]

Introduction

Multiple myeloma is a malignancy of plasma cells that reside primarily in the bone marrow. Although initially responsive to many chemotherapeutic agents, patients with multiple myeloma frequently experience disease relapse that is resistant to multiple drugs and ultimately incurable in most cases (1). With the use of high-resolution, genome-wide molecular genetic analyses done on large, uniformly treated patient cohorts, several genetic entities defining disease subtypes are emerging (2, 3). One of the most consistent findings in these studies is the amplification and overexpression of genes, especially CDC28 protein kinase regulatory subunit 1B (*CKS1B*), localized to chromosome 1q21. We and others have shown a strong correlation between a poor prognosis and gain/amplification of chromosome arm 1q21 (2, 4, 5). To identify antineoplastic agents with activity in tumors with this high-risk molecular marker, we used the COMPARE algorithm (http://dtp.nci.nih.gov; ref. 6), which identifies correlations between gene expression patterns and drug activity (7–10). By this approach, we identified ellipticines and several other synthetic compounds that showed a strong correlation between their median growth inhibition (GI_{50}) in the NCI-60 human tumor cell lines (11) and *CKS1B* expression. We subsequently investigated the cytotoxic activity of >20 of these compounds and found that 9-dimethyl amino-ethoxy ellipticine (NSC 338258 or EPED3) is a highly effective *in vitro* antimyeloma agent. EPED3 is a hydrophilic derivative of ellipticine (Fig. 1), a hydrophobic cell-permeable alkaloid originally derived from Apocyanaceae plants (12).

Ellipticine is a polycyclic molecule that intercalates between DNA base pairs and induces G_2-M-phase cell cycle arrest (13). Previous molecular studies suggested that ellipticine acted primarily through its binding to nucleic acids and inhibition of *topoisomerase II* (*topo II*) and topo II–mediated DNA damage (14). Cytochrome *P*450-dependent oxidation at the 7- or 9-carbon position has been shown to promote DNA intercalation and adduct formation, thereby enhancing the cytotoxic potential of these agents (15). Additionally, selection for ellipticine resistance in a Chinese hamster lung cell line resulted in a phenotype that was cross-resistant to all known topoisomerase-targeting agents as well as several additional *P-glycoprotein* substrates (16, 17). More recently, Vendôme et al. (18) investigated the potential of ellipticine analogues as tyrosine kinase inhibitors and found that a mutant *c-kit kinase* activity could be inhibited by ellipticine derivatives with substitutions at the 9-carbon position. The ellipticine derivative EPED3 was not examined in this study, although a structure-activity relationship analysis showed that agents with groups at the C-9 position that could form a hydrogen bond were the most active. Using COMPARE to correlate the cytotoxic activity of EPED3 and other ellipticine derivatives with gene expression, Huang et al. (19) suggested

Received 8/2/07; revised 12/4/07; accepted 2/1/08.

Grant support: NIH grants CA55819 (J.D. Shaughnessy, Jr. and B. Barlogie) and CA97513 (J.D. Shaughnessy, Jr.), Fund to Cure Myeloma, and Nancy and Stephen Grand Philanthropic Fund.

The costs of publication of this article were defrayed in part by the payment of page charges. This article must therefore be hereby marked *advertisement* in accordance with 18 U.S.C. Section 1734 solely to indicate this fact.

Requests for reprints: John D. Shaughnessy, Jr., The Donna D. and Donald M. Lambert Laboratory of Myeloma Genetics, Myeloma Institute for Research and Therapy, University of Arkansas for Medical Sciences, Little Rock, AR. E-mail: shaughnessyjohn@umas.edu

doi:10.1158/1535-7163.MCT-07-0524

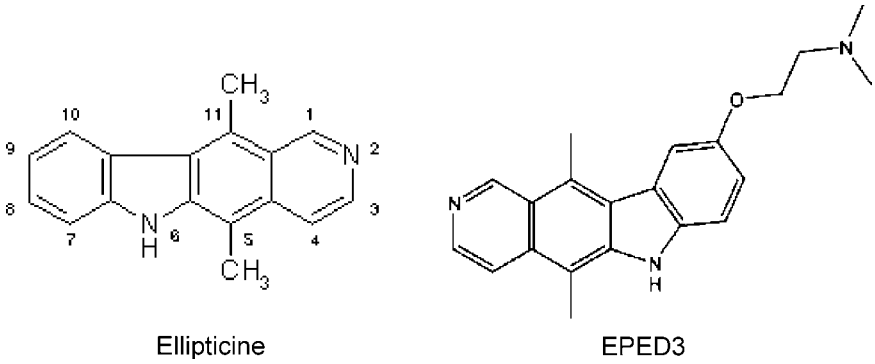

Figure 1. Chemical structures of ellipticine and EPED3. EPED3 (*right*), a water-soluble derivative of ellipticine (*left*), with a substitute radical of dimethyl amino-ethoxy at the C-9 position.

that EPED3 might inhibit *multiple drug-resistant protein 1/P-glycoprotein*–mediated drug efflux. Thus, the molecular target of EPED3 and its mechanism of action as an antineoplastic agent are largely unknown. Because of our interest in developing agents for treating molecularly defined high-risk multiple myeloma, we conducted *in vitro* experiments in clinically relevant settings. The disease relies on dynamic interactions between myeloma cells and bone marrow–derived stromal cells, and this interaction can protect malignant cells from drug-induced apoptosis (20). With this in mind, we examined EPED3 cytotoxicity in myeloma cell lines cocultured with stromal cells to simulate the *in vivo* setting. In these coculture conditions, low concentrations of EPED3 caused rapid cell cycle arrest and massive apoptosis of myeloma cells, whereas stromal cells remained viable.

Materials and Methods

Cell Lines and Culture

The human myeloma cell lines H929, OPM-2, RPMI-8226, and U266 were purchased from the American Type Culture Collection. The ARK myeloma cell line was developed in our laboratories, and the remaining myeloma cell lines were kindly provided by Dr. Michael Kuehl (Genetics Department, Medicine Branch, National Cancer Institute). The RPMI-8226/Dox1V drug-resistant variant was the kind gift of Dr. William S. Dalton (H. Lee Moffitt Cancer Center) and is maintained under chronic selective pressure (1×10^8 mol/L doxorubicin and 10 μg/mL verapamil; Sigma-Aldrich). The cell line is characterized by reduced expression and activity of *topo II* and shows cross-resistance to other *topo II* poisons, such as mitoxantrone and etoposide; however, it is not resistant to chemotherapeutic agents not known to target *topo II*, including melphalan, vincristine, cytarabine, and dexamethasone (21). HS-5 (American Type Culture Collection) is a long-term human bone marrow stromal cell line transformed with human papillomavirus.

All cell lines were maintained in RPMI 1640 (Invitrogen) supplemented with 10% fetal bovine serum (Atlanta Biological), 100 units/mL penicillin/streptomycin, 2 mmol/L L-glutamine, and 1 mmol/L sodium pyruvate (Invitrogen). Cells were incubated at 37°C with 5% carbon dioxide.

In vitro Screening of DPT Compounds

Myeloma cell lines were maintained at >90% viability and seeded in 96-well tissue culture plates at 10^3 cells per well in a 50 μL aliquot. All compounds obtained from the Developmental Therapeutics Program (DTP) of the National Cancer Institute were initially dissolved in 100% DMSO (Sigma-Aldrich) at 1 mg/mL, further diluted in fresh medium to 1 μg/mL, and added to each well in a 50 μL aliquot. All experiments were conducted in triplicate. With the use of the luminescent assay kit CellTiter-Glo (Promega) according to the manufacturer's instructions, cell viability was assayed every 24 h after addition of the DTP compounds for 5 days. Luminescence intensity was measured by a computerized luminometer (Promega), with each well being read five times within 30 min. The statistical sampling distribution per cell line for each compound was based on a sample of 15 measurements.

Coculture System

The monolayer of HS-5 cells were trypsinized (Invitrogen), seeded in six-well plates, and allowed to reach 75% confluence. For indirect contact coculture, myeloma cells were suspended in TC inserts with 3.0 μm pore size track-etched polyethylene terephthalate membranes (Becton-Dickinson Labware) at 10^6/mL of total volume of medium (5 mL/well) as HS-5 cells adhered to the bottom of the plates. Antimyeloma agents were added individually at serial 2-fold titration; control wells received medium only.

3-(4,5-Dimethylthiazol-2yl)-2,5-Diphenyltetrazolium Bromide Assay of Cell Proliferation

We used a 3-(4,5-dimethylthiazol-2yl)-2,5-diphenyltetrazolium bromide (MTT) reduction assay kit (Promega) to determine cell proliferation and survival. Briefly, myeloma cells were seeded in 96-well plates at 2×10^4 per well. Antimyeloma agents were diluted in a serial 2-fold titration according to the potency of each agent. All tests were set in triplicate or quadruplicate. MTT assays were done 96 h after addition of the agents by adding the dye solution to each well (15 μL/well) and further incubating at 37°C and 5% carbon dioxide for 2 h; the reactions were then stopped with 100 μL of the solubilization solution/stop mix. Plates were read

simultaneously at wavelengths of 570 and 650 nm in a plate reader; the A_{570} values were corrected by the A_{650} values.

Flow Cytometry Analyses

Cell cycle arrest was measured with the use of the DNA-Prep Reagent System kit (Beckman Coulter). Myeloma cells were harvested from coculture TC inserts and washed in PBS; 5×10^5 cells were stained according to the manufacturer's instructions. Samples were analyzed with the EPICS XL-MCL flow cytometer equipped with EXPO32 ADC software (Beckman Coulter).

Apoptosis was detected by staining with Annexin V-FITC (Beckman Coulter). Myeloma cells were harvested from coculture TC inserts and washed in PBS; 5×10^5 cells were incubated on ice with 100 μL binding buffer and 10 μL Annexin V-FITC for 15 min. Samples were analyzed with the EPICS XL-MCL flow cytometer equipped with EXPO32 ADC software (Beckman Coulter).

Mitochondria and Cytochrome *c* Staining

Myeloma cells were in TC inserts cocultured with HS-5 cells and treated with individual antimyeloma agents. An aliquot containing 10^6 cells was transferred to a 24-well plate and mixed with MitoTracker Red CMXRos (Invitrogen) at a 50 nmol/L final concentration. After 15 min, cells were collected, washed with PBS, and adhered to slides (5×10^4 per spot) by Shandon-Cytospin centrifugation (Thermo Electron). Slides were fixed in 3.7% formaldehyde/PBS for 15 min and rinsed in PBS; the cells were permeabilized in ice-cold acetone for 5 min and rinsed twice in a solution of PBS with 0.1% NP-40 (PBD). Mouse antihuman cytochrome *c* monoclonal antibody (R&D Systems) was diluted 1:500 with 10 mmol/L Na^+PO_4 (pH 7.8)/0.15 mol/L NaCl buffer and added to each spot. After 15 min, slides were washed twice in PBD. FITC-conjugated goat anti-mouse IgG H+L chain (BD Biosciences) was added, and slides were

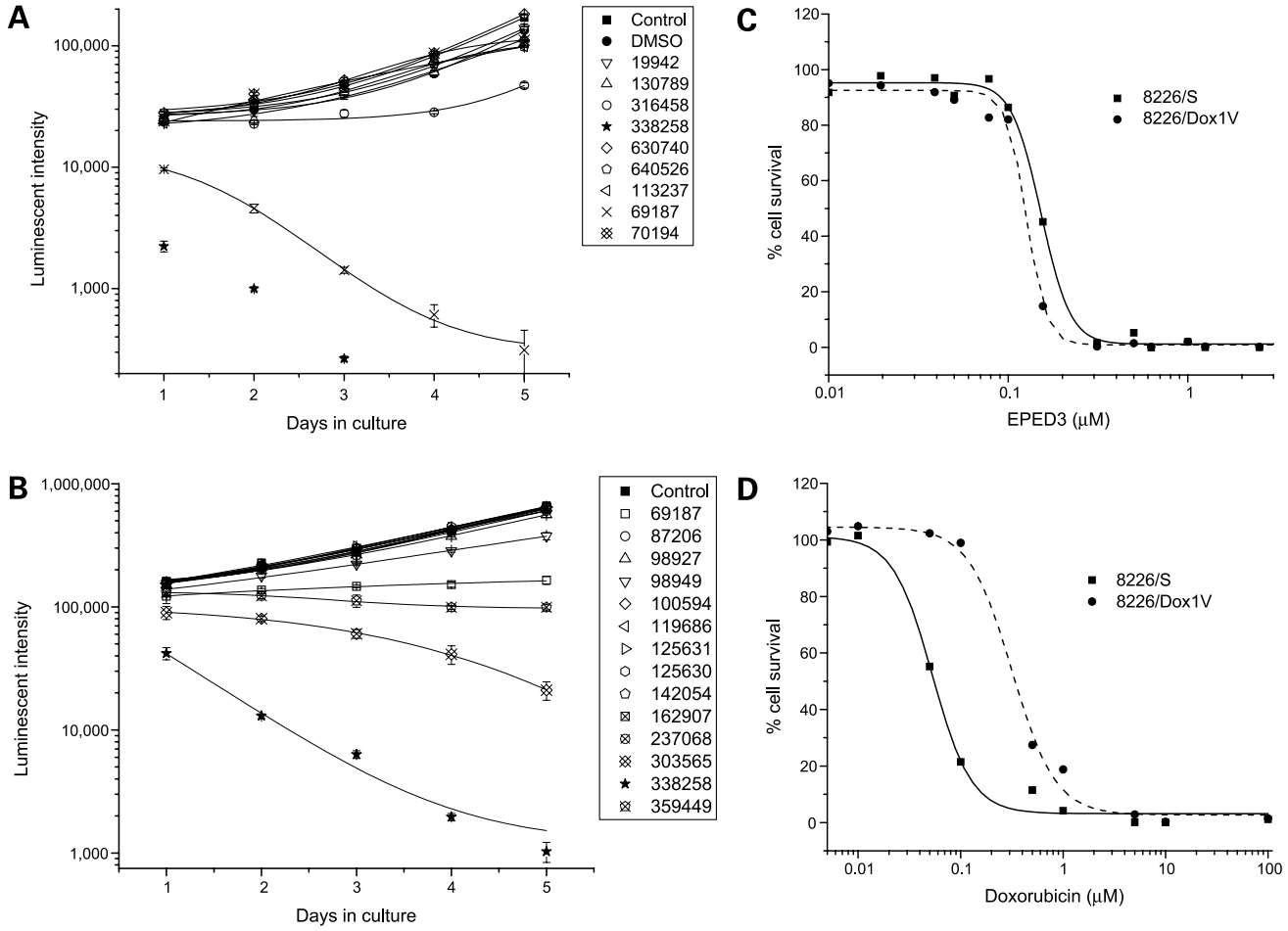

Figure 2. Screening process identified high antimyeloma efficacy of EPED3 and dose response of RPMI-8226 and RPMI-8226/Dox1V myeloma cells to EPED3 or doxorubicin. **A,** U266 myeloma cell line was treated with nine DTP compounds (Supplementary Table S1)[3] at 0.5 μg/mL for 5 d. Cell viability was measured every 24 h with the CellTiter-Glo luminescent assay. The luminescent intensity is plotted as a function of time. **B,** U266 cells were treated with 14 different ellipticine derivatives at 0.5 μmol/L for 5 d. Ellipticine derivatives are coded with NSC identifiers, and NSC 338258 was later renamed as EPED3. Cell viability was plotted as a function of time. **C,** linear regression analysis of the IC_{50} values for EPED3- or doxorubicin-treated RPMI-8226 (*solid lines/squares*) and RPMI-8226/Dox1V (*dashed lines/diamonds*). Mean of four independent experiments. RPMI-8226/Dox1V (*8226/Dox1V*) cells showed no significant resistance to EPED3 comparing with the parental line (*8226/S*). In contrast (**D**), in response to doxorubicin, 8226/Dox1V cells exhibited 7.3-fold higher resistance than 8226/S. $P < 0.0001$.

Table 1.

(A) IC_{50} of EPED3, Alkeran, and bortezomib to myeloma cell lines

Cell lines	EPED3 (μmol/L)	EPED3 (μmol/L) with 2% human serum albumin*	Alkeran† (μmol/L)	Bortezomib (nmol/L)
	IC_{50}‡ ± SE	IC_{50} ± SE	IC_{50} ± SE	IC_{50} ± SE
JJN3	0.68 ± 0.01	0.59 ± 0.03	2.83 ± 0.95	3.37 ± 0.15
Ark	0.43 ± 0.26	0.22 ± 0.02	2.50 ± 0.20	3.79 ± 0.58
KMS11	0.43 ± 0.01	0.29 ± 0.01	11.47 ± 7.13	2.86 ± 0.11
ANBL6	0.42 ± 0.01	0.19 ± 0.00	10.10 ± 1.24	1.73 ± 0.05
H929	0.38 ± 0.01	0.25 ± 0.00	2.86 ± 0.04	1.84 ± 0.09
OCI-MY1	0.30 ± 0.03	0.17 ± 0.01	8.06 ± 1.58	0.15 ± 0.17
L363	0.28 ± 0.01	0.22 ± 0.01	1.43 ± 0.66	3.00 ± 0.05
INA6	0.23 ± 0.03	0.22 ± 0.01	1.01 ± 0.09	3.64 ± 0.13
MM144	0.18 ± 0.01	0.17 ± 0.01	1.15 ± 0.17	0.10 ± 0.13
RPMI-8226	0.12 ± 0.01	0.16 ± 0.00	4.90 ± 1.06	0.20 ± 0.12
U266	0.11 ± 0.01	0.11 ± 0.01	17.03 ± 6.36	0.23 ± 0.08
OPM-2	0.10 ± 0.01	0.16 ± 0.01	11.68 ± 5.96	0.33 ± 0.04

(B) IC_{50} of EPED3 on myeloma cell lines with or without HS-5 cell coculture

Cell lines	Myeloma cells and HS-5 cells in coculture	Myeloma cells
	IC_{50} ± SE of EPED3 (μmol/L)	IC_{50} ± SE of EPED3 (μmol/L)
JJN3	2.20 ± 0.62	0.68 ± 0.01
Ark	1.04 ± 0.16	0.43 ± 0.26
KMS11	1.15 ± 0.14	0.43 ± 0.01
ANBL6	1.17 ± 0.08	0.42 ± 0.01
H929	0.87 ± 0.03	0.38 ± 0.01
OCI-MY1	1.29 ± 0.12	0.30 ± 0.03
L363	0.41 ± 0.86	0.28 ± 0.01
INA6	0.50 ± 0.69	0.23 ± 0.03
MM144	0.60 ± 0.00	0.18 ± 0.01
RPMI-8226	0.83 ± 0.04	0.12 ± 0.01
U266	0.52 ± 0.08	0.11 ± 0.01
OPM-2	0.21 ± 0.44	0.10 ± 0.01

*Myeloma cell lines were treated with EPED3 in complete medium containing 2% human serum albumin.
†Alkeran (melphalan hydrochloride) was dissolved in nonpyrogenic diluent immediately before *in vitro* drug titration.
‡IC_{50} (50% inhibitory concentration of an agent) was calculated using sigmoidal-fit function of OriginPro 7.5 software.

incubated 15 min. Finally, to stain cell nuclei, slides were incubated with 0.1 μg/mL 4,6-diamidino-2-phenylindole (Sigma-Aldrich) in PBS and mounted with Antifade solution (Invitrogen). Images were captured with the use of the Genetic Workstation, with a red (for mitochondrial staining), green (for cytochrome *c* staining), and blue (for nuclear staining) single band-pass filter set (Abbot Vysis).

Western Blotting and Detection

Myeloma cell lines were indirectly cocultured with HS-5 cells as described above. EPED3 or bortezomib (Millennium Pharmaceuticals) was added to cocultures to final concentrations of 2 and 0.5 μmol/L, respectively. After 6 h of treatment, myeloma cells were harvested from the inserts, washed twice in PBS, and resuspended at 10^4 cells/μL in protein extraction buffer [PBS with 10 μg/mL aprotinin, 10 μg/mL leupeptin, and 1 mmol/L phenylmethylsulfonyl fluoride (Sigma-Aldrich)]. Cell lysates were prepared by three cycles of freezing in liquid nitrogen followed by thawing at 37°C. Protein concentration was determined by spectrophotometry (NanoDrop Technologies).

For SDS-PAGE, 100 μg protein extract was mixed with NuPAGE LDS sample buffer (Invitrogen) and loaded into each lane of the gel (10-15% polyacrylamide separating gel, 4% stacking gel). After electrophoresis, protein was transferred to Hybond ECL nitrocellulose membrane (Amersham Pharmacia Biotech). Primary goat anti-human *caspase-3, caspase-8*, and *caspase-9* polyclonal antibodies (R&D Systems), rabbit anti-human *CKS1B*, and mouse anti-human *β-tubulin* (Invitrogen) were applied and then detected with the WesternBreeze Western blot immunodetection kits (Invitrogen) according to the manufacturer's instructions.

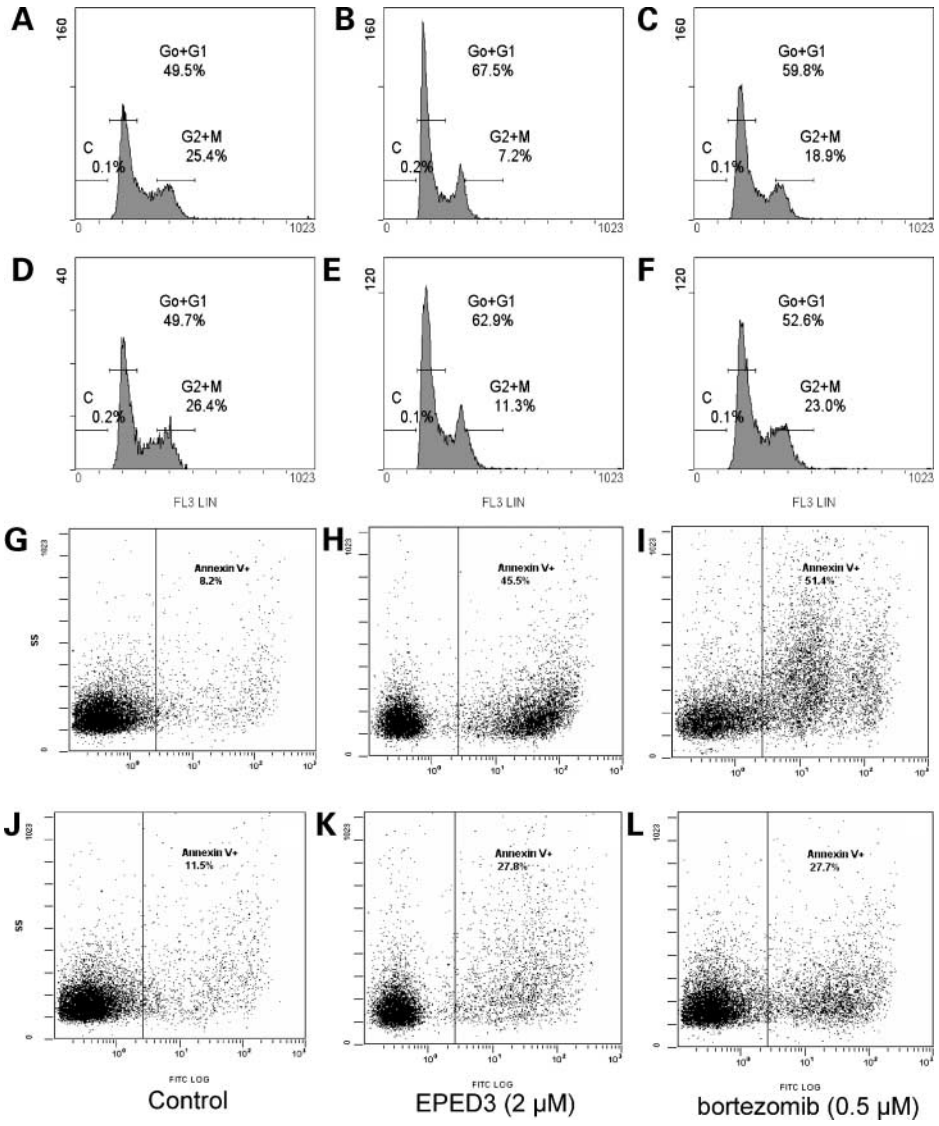

Figure 3. Flow cytometric analyses of cell viability and cell cycle arrest with EPED3 and bortezomib treatment. U266 cells were cocultured with indirect contact with HS-5 cells for 12 h. Cells were untreated or exposed to 2 μmol/L EPED3 or 0.5 μmol/L bortezomib. Pan-caspase inhibitor Z-VAD-FMK (50 μmol/L) was also added to cocultures (**D**-**F** and **J**-**L**) to block caspase-dependent apoptosis. **A** to **F,** U266 cells were harvested and analyzed for cell cycle arrest by flow cytometry. Cells in G_0-G_1 and G_2-M phases were measured (%) by the area under the peaks corresponding to DNA content and were gated with each graph; the cells with fragmented DNA are indicated as C% in each graph. **G** to **L,** cells were analyzed for apoptotic status with an Annexin V-FITC kit. Viable cells (control) were gated in the left. Apoptotic cells were gated as Annexin V positive. **K** and **L,** EPED3- or bortezomib-induced apoptosis was blocked by adding Z-VAD-FMK.

Electron Microscopy Study of Apoptosis Induced by EPED3

U266 myeloma cells (10^6/mL) were treated for 6 h with 2 μmol/L EPED3. Cells were harvested, washed twice in PBS, and then fixed in 3% glutaraldehyde solution; postfixation with 1% osmium tetroxide followed. After serially graded ethyl alcohol dehydration, cells were embedded in resin (Embed 812, Electron Microscopy Sciences) and baked overnight at 60°C for polymerization; sectioning then followed. The morphology of U266 cells was examined and captured with a transmission electron microscope (Philips Electronics; ref. 22).

Results

EPED3 Showed Significant Antineoplastic Activity among All Tested DTP Compounds

To identify potential anticancer compounds with specific potency in cells with high-risk molecular features, we used the National Cancer Institute's COMPARE program to query growth inhibition data in the DTP open database of ~44,000 synthetic compounds. The GI_{50} value (the concentration that causes 50% growth inhibition) of a compound was used as the selection criterion for this analysis.

Initially, 24 DTP compounds (Supplementary Table S1)[3] were identified by a strong correlation of cytotoxicity with expression levels of the gene *CKS1B*, a high-risk feature in multiple myeloma, in the NCI-60 cancer cell panel. These compounds were screened for effectiveness against four myeloma cell lines: ARK, KMS11, RPMI-8226, and U266. The compounds were added to cells at a final concentration 0.5 μg/mL. Cell viability was determined with CellTiter-Glo assays every 24 h over the following 5 days and compared with untreated controls (medium

[3] Supplementary material for this article is available at Molecular Cancer Therapeutics Online (http://mct.aacrjournals.org/).

only or 0.5% DMSO). Two ellipticine derivatives, EPED3 and NSC 69187, most significantly inhibited cell viability in the four myeloma cell lines (Fig. 2A). With this finding in hand, we extended our study to additional ellipticine derivatives from the DTP. A substantial number of ellipticine derivatives had significant Pearson correlation coefficients, indicating the general tendency of the compound toward cell-killing activity in association with high *CKS1B* gene expression levels in the NCI-60. Among the ellipticines with high Pearson correlation coefficients, we focused on those with a high SD, which measures the degree of difference in the response of the cell line to the compound of interest. Of 18 ellipticines listed in Supplementary Table S2,[3] we tested 12 compounds (insoluble ellipticines were excluded) for growth inhibition of the same four cell lines. The data indicated that, among the ellipticine derivatives, EPED3 most significantly inhibited myeloma cell growth (Fig. 2B). This suggests that the enhanced antineoplastic activity of EPED3 is related to the specific modifications made to produce EPED3 (Fig. 1).

The cytotoxicity of EPED3 was further tested with a panel of 12 myeloma cell lines in a serial 2-fold titration (50-3,200 nmol/L). Two commonly used antimyeloma agents, melphalan (Alkeran; Celgene) and bortezomib (Velcade, Millennium Pharmaceuticals), were simultaneously set for direct comparison at concentrations ranging from 2 to 128 μmol/L and 0.5 to 32 nmol/L, respectively. Cytotoxicity was analyzed by MTT assay. Absorbance was read after 96-h incubation, and the 50% inhibitory concentration (IC_{50}) of EPED3, melphalan, or bortezomib for each myeloma cell line was calculated with the use of OriginPro 7.5 software (OriginLab). EPED3 inhibited myeloma cell growth at nanomolar concentrations in all cell lines tested (Table 1A). Additionally, to determine whether human serum albumin would affect drug activity in future clinical trials, MTT assays were done in the presence of 2% human serum albumin. No inhibition of cytotoxicity was seen in these assays.

EPED3 Cytotoxicity Is Reduced by Coculture with Stromal Cells

Previous studies showed that bone marrow–derived stromal cells contributed to the survival of multiple myeloma cells via both soluble factors and direct cell contact (20, 23, 24). To determine the effect of the sensitivity of myeloma cells to EPED3 in the presence of protective stromal cells, we treated 12 myeloma cell lines in coculture with HS-5 cells. EPED3 was diluted in a 2-fold series (range, 125-4,000 nmol/L). Myeloma cell

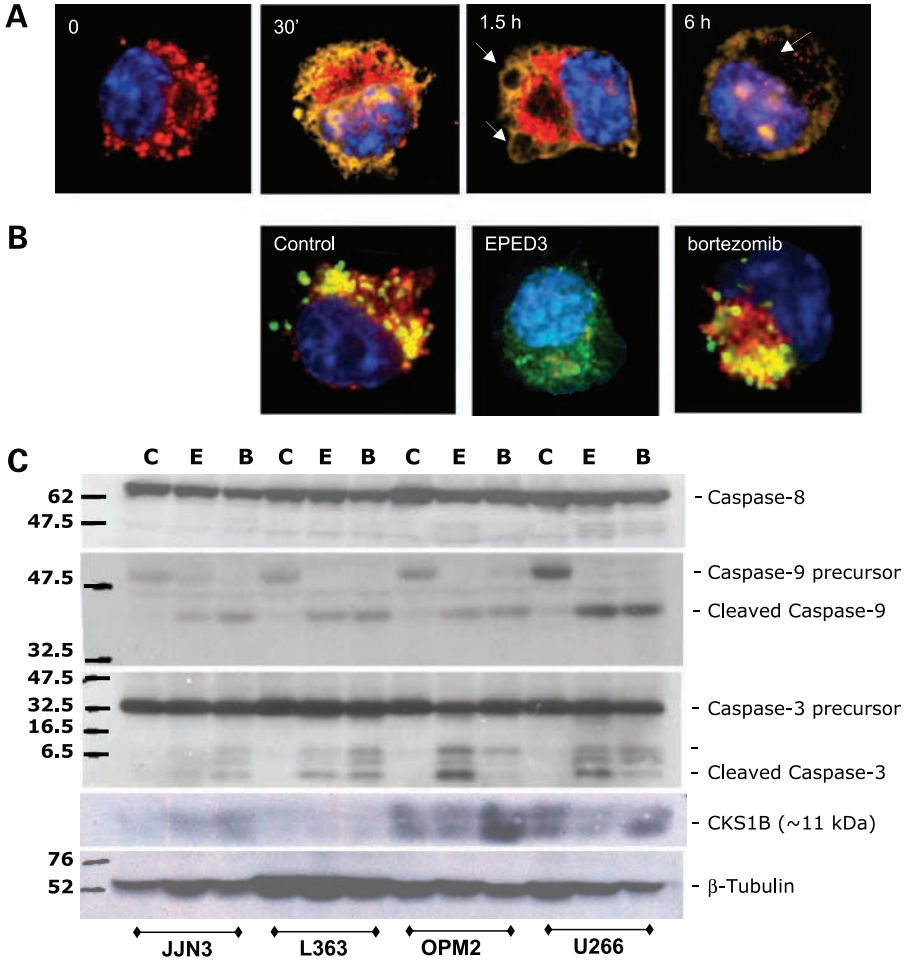

Figure 4. EPED3 distribution throughout the cytoplasm and induction of apoptosis. U266 cells were cocultured with indirect contact with HS-5 cells and treated with EPED3 (2 μmol/L) or bortezomib (0.5 μmol/L). For analysis by fluorescence microscopy, nuclei were stained with 4,6-diamidino-2-phenylindole (*blue*), mitochondria with MitoTracker Red CMXRos (*red*), and cytochrome *c* with monoclonal antibody/FITC-secondary antibodies (*green*). EPED3 was excited by UV light and was visualized as gold. **A,** cells were photographed under fluorescence microscopy at the time of treatment and 30 min, 1.5 h, and 6 h thereafter (×600). The appearance of large cytoplasmic vacuoles (*arrows*) and diminished mitochondria in cells treated with EPED3 indicate ongoing apoptosis. **B,** cells treated with EPED3 and bortezomib were examined after 6 h for mitochondrial lysis and cytochrome *c* release (*green*). Cytochrome *c* disassociation from mitochondria indicates initiation of the intrinsic apoptotic pathway (×600). **C,** myeloma cell lines (JJN3, L363, OPM-2, and U266) were cocultured with indirect contact with HS-5 cells and treated with EPED3 (2 μmol/L) or bortezomib (0.5 μmol/L) for 6 h. Protein extracts (100 μg) were analyzed by Western blotting method with goat anti-human *caspase-3, caspase-8*, and *caspase-9* polyclonal antibodies, rabbit anti-human *CKS1B* antibody, and mouse anti-human *β-tubulin* antibody, respectively. C, medium control; E, EPED3; B, bortezomib.

proliferation was determined with MTT assays 96 h after the addition of EPED3. From each TC insert, myeloma cells were homogenously suspended, and aliquots were transferred to a 96-well plate for MTT assay. The adherent HS-5 cells were simultaneously assayed by MTT dye reduction after removal of the TC inserts from each plate (n = 12). The IC_{50} values of EPED3 in each myeloma cell line, as well as HS-5 cells, were calculated with OriginPro 7.5 software (Table 1A; Supplementary Fig. S1).[3] Myeloma cell lines showed a mean 3.2-fold resistance (range, 1.46-6.92 μmol/L increase of IC_{50}; Table 1B) to EPED3 in coculture with HS-5 stromal cells compared with myeloma cells alone. HS-5 cells showed no significant cell death at the highest dose of EPED3 examined (Supplementary Fig. S1).[3] The cytotoxicity of EPED3 to HS-5 cells was also tested without the presence of myeloma cells. HS-5 cells were initially seeded in 96-well TC plates at 2-fold incremental densities and exposed to serially diluted EPED3 for 96 h. The MTT assays indicated that HS-5 cells at higher density were more insensitive to EPED3 (Supplementary Fig. S2).[3]

EPED3 Was a Highly Effective Antimyeloma Agent That Inhibited Myeloma Cell Proliferation and Overcame Acquired Drug Resistance

The cytotoxicity of EPED3 was compared *in vitro* with those of ellipticine and four other, commonly used antimyeloma agents in four myeloma cell lines: JJN3, L363, OCI-MY5, and U266. Ellipticine, doxorubicin, etoposide, dexamethasone, bortezomib, and EPED3 were each applied in a 2-fold dilution series at concentrations ranging from 0.1 to 6.4 μmol/L. Cell proliferation was assessed with MTT assays 24 and 48 h after initiation of treatments. In contrast to all other agents, except bortezomib, area-under-the-curve calculations indicated that EPED3 efficacy was dose dependent but not time dependent (Supplementary Table S3).[3]

Because ellipticine has been reported to inhibit *topo II* and *in vitro* selection for ellipticine resistance is reported to result in a phenotype with cross-resistance to topoisomerase-targeting agents, we examined the activity of EPED3 in a drug-resistant variant of the RPMI-8226 myeloma cell line. The RPMI-8226/Dox1V cell line was selected for resistance to doxorubicin in the presence of the ATPase inhibitor verapamil. This selection scheme prevents the emergence of P-glycoprotein-mediated multidrug resistance. Rather, resistance is due to a reduction in the expression and activity of *topo IIα*. RPMI-8226/Dox1V cells and the parental line (RPMI-8226) were each incubated with serial dilutions of EPED3 or doxorubicin, as described previously (21), and cell growth was assessed with MTT assays. Linear regression analysis of 96-h dose-response curves was used to compare the cytotoxic activity of EPED3 in RPMI-8226/Dox1V and RPMI-8226 cells. EPED3 cytotoxicity in the doxorubicin-resistant myeloma cells was not

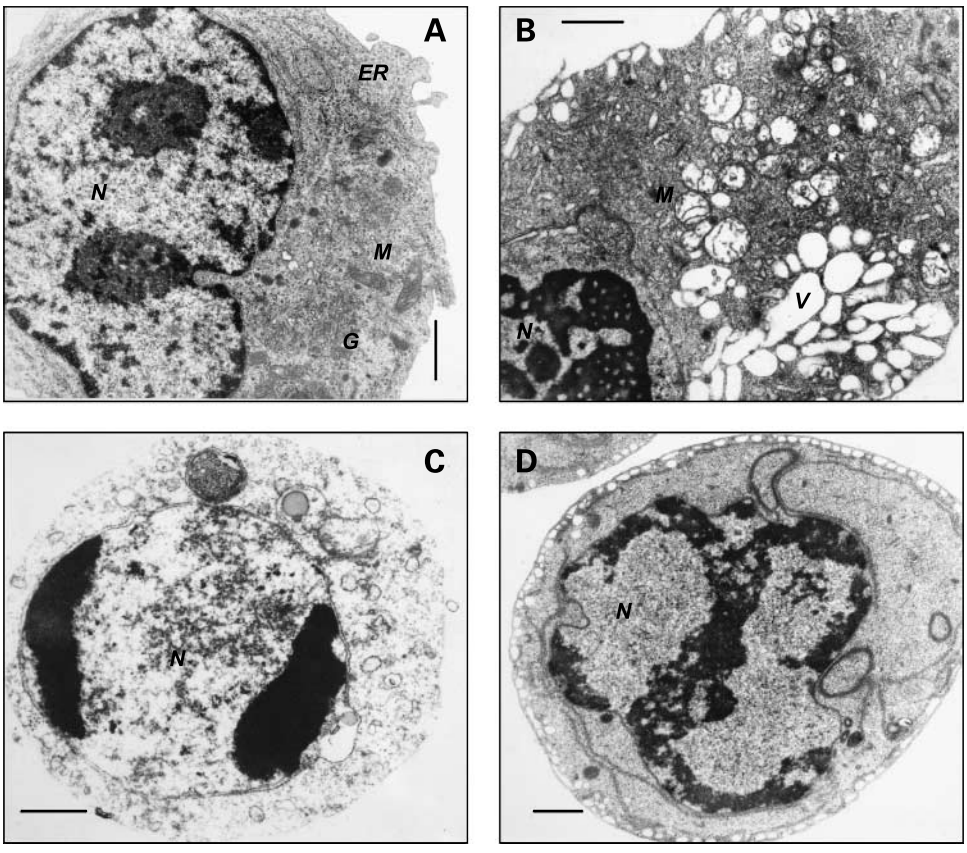

Figure 5. Ultrastructural observation of EPED3-induced apoptosis of U266 cells. U266 cells were treated with EPED3 (2 μmol/L) for 6 h, fixed in 3% glutaraldehyde solution, and stained with 1% osmium tetroxide. **A,** ultrastructure of an untreated U266 cell depicts the characteristics of plasma cells with a large nucleus (*N*), well-developed Golgi apparatus (*G*), mitochondria (*M*), and endoplasmic reticulum (*ER*). **B** to **D,** EPED3-treated U266 cells underwent apoptotic processes reflected in pyknosis (a condensation and reduction in the size of the nucleus, usually associated with hyperchromatosis), severely damaged mitochondria with destruction of inner cristae (*B*), and formation of numerous vacuoles (*V*). With EPED3 treatment, typical apoptosis is marked by degeneration of organelles and rupture of the cytoplasmic membrane. Bar, 1 μm.

significantly different from its activity in the parental cells (mean IC_{50}, 131.3 ± 36.0 nmol/L, $n = 4$, versus 150.3 ± 40.6 nmol/L, $n = 4$, respectively; $P = 0.7$; Fig. 2C). In contrast, RPMI-8226/Dox1V cells showed 7.3-fold higher resistance to the cytotoxic effects of doxorubicin, a known topo II inhibitor, than did parental RPMI-8226 cells (IC_{50}, 293.5 ± 34.01 nmol/L, $n = 4$, versus 40 ± 17.68 nmol/L, $n = 4$, respectively; $P < 0.0001$; Fig. 2D).

EPED3-Induced Apoptosis and Cell Cycle Arrest of Myeloma Cells

To investigate the effects of EPED3 on the cell cycle and apoptosis of myeloma cells, U266 cells were exposed to 2 μmol/L EPED3 or 0.5 μmol/L bortezomib in TC insert coculture with HS-5 cells. Cells were harvested and stained for DNA content or with Annexin V for flow cytometry analyses. After treating U266 myeloma cells for 12 h, we found that 67.5% of the EPED3-treated population, compared with 49.5% of the untreated control population and 59.8% of the bortezomib-treated population, was in G_0-G_1 phase. Furthermore, 7.2% of the EPED3-treated population, in contrast to 25.4% of the control population and 18.9% of the bortezomib-treated population, was in G_2-M phase (Fig. 3A-C). The addition of Z-VAD-FMK, a pan-caspase inhibitor, to the cocultures did not significantly change the cell cycle distribution of cell populations when U266 cells were exposed to EPED3 or bortezomib (Fig. 3D-F), suggesting that the reduced number of cells in G_2-M phase was not due to cell death.

Based on simultaneous flow cytometry analysis of Annexin V-FITC staining, the degree of programmed cell death resulting from EPED3 treatment at 45.5% was marginal compared with that of 51.4% with bortezomib (Fig. 3G-I). However, the cytotoxicity of both EPED3 and bortezomib was blocked by addition of Z-VAD-FMK, which resulted in decreased cell death in both EPED3-treated (27.8%) and bortezomib-treated (27.7%) cells (Fig. 3J-L). These data suggest that the cytotoxicity of both agents operates in part through caspase-dependent apoptotic mechanisms.

EPED3 Activated the Intrinsic Pathway of Cell Death

We used EPED3 autofluorescence to visually examine its intracellular distribution in myeloma cells. The EPED3 molecule emits fluorescence when exposed to UV light at a wavelength of ≤500 nm. Under fluorescence microscopy, cells that have taken up EPED3 are therefore discernible by the characteristic golden light emitted by the compound. When cells were treated with EPED3, we observed nearly instantaneous permeation, with cytosolic distribution of the agent within 15 min of exposure (data not shown). Six hours after treatment, large vacuoles formed within the cells, indicating ongoing apoptosis; disintegration of the plasma membrane, another hallmark of apoptosis, was visualized as the intensity of EPED3 fluorescence dimmed in the cytosol (Fig. 4A). The uptake of EPED3 was also found in HS-5 cells in coculture with myeloma cells (Supplementary Fig. S3).[3]

To investigate the effects of EPED3 on mitochondrial integrity and cytochrome *c*, we used immunohistochemistry. Disruption of mitochondria in EPED3-treated U266 myeloma cells was shown by the loss of staining with MitoTracker Red CMXRos and subsequent release of cytochrome *c* from the mitochondrial membrane into the cytosol. In contrast, mitochondrial disruption and cytochrome *c* release were not seen in cells similarly treated with bortezomib (Fig. 4B).

Using Western blotting, we also investigated the activation of caspases involved in the mitochondrial apoptotic pathway. JJN3, L363, OPM-2, and U266 cells were indirectly cocultured with HS-5 cells and treated with EPED3 or bortezomib for 6 h. Proteins were then extracted from myeloma cells and analyzed for activation of *caspase-8, caspase-9*, and *caspase-3*. None of the myeloma cell lines examined showed obvious activation of *caspase-8*, suggesting that the extrinsic apoptotic pathway is not involved in EPED3 cytotoxicity. In contrast, the strong activation of *caspase-9* followed by the cleavage of *caspase-3* indicated that the intrinsic apoptotic pathway was involved in triggering the proteolytic cascade in all myeloma cell lines (Fig. 4C).

EPED3 Prompted the Destruction of Mitochondria and Elicited Cell Death

Electron microscopy was used to examine subcellular morphology following EPED3 exposure. The electron microscopic observation revealed that U266 cells underwent severe degenerative changes 6 h after treatment with 2 μmol/L EPED3. Ultrastructural alterations, including pyknosis (condensation and reduction in nuclear size associated with hyperchromatosis), destruction of mitochondrial inner cristae, and formation of multiple cytosolic vacuoles, reflected the apoptotic state of the treated cells (Fig. 5).

Discussion

For ~15 years, the DTP of the National Cancer Institute has used the NCI-60 panel to screen potential anticancer agents for their ability to inhibit growth in established cancer cell lines (7). Early in this process, it was recognized that compounds with similar mechanisms had similar patterns of sensitivity. This led to development of the COMPARE algorithm (6), which compiles a list of compounds with patterns of growth inhibition similar to that of a ''seed'' compound supplied by an investigator. This approach has been useful in the investigation of potential mechanisms of action for novel compounds. More recently, molecular characterization of the NCI-60 has provided an opportunity to apply COMPARE analysis to gene expression signatures (9, 10). In the present study, the COMPARE algorithm was used to correlate gene expression profiles with the potency of anticancer compounds (10). Correlation of the expression levels of the *CKS1B* gene, whose overexpression is associated with rapid failure of high-dose therapies (25), with the activity of antineoplastic agents in the in the NCI-60 panel led to the identification of EPED3 as a potential new, rationally identified antimyeloma agent.

EPED3 is an analogue of ellipticine with a dimethyl amino-ethoxy substitution at the C-9 position. This radical

not only tremendously improves the hydrophilicity of the compound, allowing rapid cellular uptake, but also prevents intracellular metabolism by the hydroxylation at C-9 of ellipticine (14). Although initially categorized as a topo II inhibitor that localizes to the nucleus, ellipticine has more recently been shown to localize in the cytoplasm and accumulate in mitochondria (26). Similarly, EPED3, which displays intrinsic fluorescence identical to ellipticine, was found to rapidly accumulate in the mitochondria in this study. Fluorescence microscopy studies show that cellular uptake of EPED3 is rapid and unrestrained. Under timed observations, EPED3 passively crosses the plasma membrane and becomes evenly distributed throughout the cytosol within minutes, suggesting that EPED3 is a lipophilic molecule that crosses the plasma membrane independent of receptor or ion channel mechanisms. Subsequent to its entry into cells, EPED3 immediately initiates an enormous loss of mitochondrial membrane potential, release of cytochrome *c*, and formation of large vacuoles (Figs. 4 and 5). The CellTiter-Glo assay, which principally quantifies ATP and signals metabolic activity, showed that EPED3-treated cells produce the lowest ATP level than all agents tested (data not shown), suggesting an inhibition of cellular chemical energy production following treatment. It is likely that, like ellipticine, EPED3 localizes to the mitochondrial inner membrane, thereby disrupting the membrane potential by uncoupling mitochondrial oxidative phosphorylation and crippling energy production in the cell. The exact mechanism of mitochondrial membrane permeability transition is not yet fully defined but may involve the generation of reactive oxygen species (data not shown).

The bone marrow microenvironment augments myelomagenesis and can protect myeloma cells from apoptosis (20, 27, 28). Although most myeloma cell lines were initially cultivated from either peripheral blood (e.g., L363, LP-1, OPM-2, RPMI-8226, and U266) or pleural effusion (e.g., ARK, ARP1, CAG, EJM, and H929), all encode the common genetic mutations that exist in primary myeloma (29). *In vitro*, soluble factors generated by intracellular interactions have been documented to contribute to protecting myeloma cells from chemotherapeutic agents (20). Thus, we used an indirect myeloma cell-stromal cell coculture system in our systematic screen to discover new synthetic compounds capable of overcoming the soluble factors present in the bone marrow microenvironment that confound therapeutic efficacy. HS-5, a long-term stromal cell line that can support the proliferation of hematopoietic progenitor cells in coculture conditions, was initially tested to better understand the activity of EPED3. HS-5 cells were set at incremental density and treated by EPED3 in 2-fold titration. Our results indicate that HS-5 cells respond to EPED3 only at high dosage and display confluence-dependent resistance as is reported for many cell lines (30).

Acquired drug resistance is a major obstacle to sustained successes in myeloma treatment. Understanding the cytotoxic mechanism of a putative therapeutic agent will allow the design of therapeutic strategies to overcome acquired drug resistance in patients. *In vitro* selection has historically been used to establish model systems for investigating the mechanisms of acquired drug resistance commonly seen in patients (30, 31). Our data indicate that EPED3 can overcome acquired drug resistance in myeloma cells selected for resistance to doxorubicin in the presence of the *P-glycoprotein* inhibitor verapamil. RPMI-8226/Dox1V cell line is cross-resistant to a variety of *topo II*–dependent therapeutic agents presumably due to reduction of *topo II* expression as well as activity (21). The cells exhibited a high tolerance to doxorubicin (Fig. 2D), which functions through *topo II* inhibition, but EPED3 treatment resulted in prompt, dose-dependent killing of RPMI-8226/Dox1V cells. Collectively, these data accentuate the much greater potency of EPED3 in killing myeloma cells, even those insensitive to topo II inhibitors, through *topo II*–dependent and time-independent mechanisms.

Dose-response analysis indicated that the efficacy of EPED3 was not schedule dependent, whereas doxorubicin is well known to be most effective in the DNA synthesis (S) phase. The IC_{50} and the area under the curve of myeloma cells responding to doxorubicin declined as drug exposure was prolonged, whereas the IC_{50} and the area under the curve of EPED3 were steady during the time course (Supplementary Table S3).[3]

Two other ellipticine derivatives that are clinically administered in the treatment of breast cancer, Celiptium (NSC 264137) and Detalliptinium (NSC 311152), also appear to act independently of topo II. DNA cleavage activity of both these ellipticine derivatives was compared *in vivo* with that of 4-(9-acridinylamino)-methanesulfonic-*m*-anisidide, a putative *topo II* inhibitor. Although IC_{50} dosages of all three agents were within close range, Celiptium and Detalliptinium were 50 times less potent for DNA strand breakage than 4-(9-acridinylamino)-methanesulfonic-*m*-anisidide (14). This is consistent with our finding that the cytotoxicity of the ellipticine derivative EPED3 is *topo II* independent.

Flow cytometry analyses in our studies showed that myeloma cells accumulate in the G_0-G_1 phase with EPED3 treatment. The mechanism of cell cycle arrest is not yet known but may be related to intracellular energy depletion. Although a high *CKS1B* gene expression profile was the initial ''seed'' in our search for more effective antimyeloma agents, the gene expression profiling results showed no significant changes in *CKS1B* gene expression after myeloma cells were exposed to 2 μmol/L EPED3 for 6 h.[4] For confirmation, we conducted Western blotting assays and found that *CKS1B* protein levels were unchanged in myeloma cell lines treated with EPED3 (Fig. 4C). These data suggest that the gene transcription or mRNA stability of *CKS1B* is not a primary target of EPED3 but that myeloma cells with *CKS1B* gene expression signature are more likely to be sensitive to EPED3. Future studies employing COMPARE algorithm analyses will be aimed

[4] E. Tian, unpublished data.

at using multiple gene expression signatures of high-risk myeloma instead of the single gene signature. Overall, multiple *in vitro*–derived lines of evidence point to reduced cell viability, cell cycle arrest, and apoptosis in myeloma cells treated with EPED3.

Acknowledgments

We thank the DTP of the National Cancer Institute for providing the synthetic compounds in this study; Simona Colla, Sushil Gupta, Yongsheng Huang, Bob Kordsmeier, Chris Randolph, Peter Stewart, Yan Xiao, David Williams, Hong Wei Xu, and Fenghuang Zhan (Donna D. and Donald M. Lambert Laboratory of Myeloma Genetics) as well as the physicians and nurses at the Myeloma Institute for Research and Therapy for contributions to establishing and maintaining the multiple myeloma gene expression profile database since 1999; the Office of Grants and Scientific Publications at the University of Arkansas for Medical Sciences for excellent editorial assistance; and Profs. Dehui Chen and Shaojun Liu and Yi Yang (Institute of Basic Medical Sciences, Academy of Military Medical Sciences, China) for their expertise in the cell ultrastructure studies.

References

1. Barlogie B, Shaughnessy J, Tricot G, et al. Treatment of multiple myeloma. Blood 2004;103:20 – 32.

2. Carrasco DR, Tonon G, Huang Y, et al. High-resolution genomic profiles define distinct clinico-pathogenetic subgroups of multiple myeloma patients. Cancer Cell 2006;9:313 – 25.

3. Zhan F, Huang Y, Colla S, et al. The molecular classification of multiple myeloma. Blood 2006;108:2020 – 8.

4. Sawyer JR, Tricot G, Lukacs JL, et al. Genomic instability in multiple myeloma: evidence for jumping segmental duplications of chromosome arm 1q. Genes Chromosomes Cancer 2005;42:95 – 106.

5. Hanamura I, Stewart JP, Huang Y, et al. Frequent gain of chromosome band 1q21 in plasma cell dyscrasias detected by fluorescence *in situ* hybridization: incidence increases from MGUS to relapsed myeloma and is related to prognosis and disease progression following tandem stem cell transplantation. Blood 2006;108:1724 – 32.

6. Zaharevitz DW, Holbeck SL, Bowerman C, Svetlik PA. COMPARE: a web accessible tool for investigating mechanisms of cell growth inhibition. J Mol Graph Model 2002;20:297 – 30.

7. Paull KD, Shoemaker RH, Hodes L, et al. Display and analysis of patterns of differential activity of drugs against human tumor cell lines: development of mean graph and COMPARE algorithm. J Natl Cancer Inst 1989;81:1088 – 92.

8. Holbeck SL, Update on NCI *in vitro* drug screen utilities. Eur J Cancer 2004;40:785 – 93.

9. Sausville EA, Holbeck SL. Transcription profiling of gene expression in drug discovery and development: the NCI experience. Eur J Cancer 2004; 40:2544 – 9.

10. Scherf U, Ross DT, Waltham M. A gene expression database for the molecular pharmacology of cancer. Nat Genet 2000;24:236 – 44.

11. Monks A, Scudiero D, Skehan P, et al. Feasibility of a high-flux anticancer drug screen using a diverse panel of cultured human tumor cell lines. J Natl Cancer Inst 1991;83:757 – 66.

12. Dalton LK, Demerac S, Elmes BC, Loder JW, Swan JM, Tertei T. Synthesis of the tumor-inhibitory alkaloids, ellipticine, 9-methoxyellipticine, and related pyrido[4,3-*b*]carbazoles. Aust J Chem 1967;20:2715 – 27.

13. Bhuyan BK, Fraser TJ, Li LH. Cell cycle phase specificity and biochemical effects of ellipticine on mammalian cells. Cancer Res 1972; 32:2538 – 44.

14. Multon E, Riou JF, LeFevre D, Ahomadegbe JC, Riou G, Top-oisomerase II-mediated DNA cleavage activity induced by ellipticines on the human tumor cell line N417. Biochem Pharmacol 1989;38:2077 – 86.

15. Stiborová M, Sejbal J, Boek-Dohalská L, et al. The anticancer drug ellipticine forms covalent DNA adducts, mediated by human cytochromes *P*450, through metabolism to 13-hydroxyellipticine and ellipticine N2-oxide. Cancer Res 2004;64:8374 – 80.

16. Larsen AK, Jacquemin-Sablon A. Multiple resistance mechanisms in Chinese hamster cells resistant to 9-hydroxyellipticine. Cancer Res 1989; 49:7115 – 9.

17. Dereuddre S, Delaporte C, Jacquemin-Sablon A. Role of topoisomer-ase IIβ in the resistance of 9-OH-ellipticine-resistant Chinese hamster fibroblasts to topoisomerase II inhibitors. Cancer Res 1997;57:4301 – 8.

18. Vendôme J, Letard S, Martin F. Molecular modeling of wild-type and D816V c-kit inhibition based on ATP-competitive binding of ellipticine derivatives to tyrosine kinases. J Med Chem 2005;48:6194 – 201.

19. Huang Y, Blower PE, Yang C, et al. Correlating gene expression with chemical scaffolds of cytotoxic agents: ellipticines as substrates and inhibitors of MDR1. Pharmacogenomics J 2005;5:112 – 25.

20. Nefedova Y, Landowski TH, Dalton WS. Bone marrow stromal-derived soluble factors and direct cell contact contribute to *de novo* drug resistance of myeloma cells by distinct mechanisms. Leukemia 2003;17: 1175 – 82.

21. Hazlehurst LA, Foley NE, Gleason-Guzman MC, et al. Multiple mechanisms confer drug resistance to mitoxantrone in the human 8226 myeloma cell line. Cancer Res 1999;59:1021 – 8.

22. Chen D, Yang H, Wang G, et al. Electron microscopic study of the morphology and morphogenesis of virus of hemorrhagic fever with renal syndrome. J Electron Microsc Tech 2005;7:111 – 7.

23. Grigorieva I, Thomas X, Epstein J. The bone marrow stromal environment is a major factor in myeloma cell resistance to dexametha-sone. Exp Hematol 1998;26:597 – 603.

24. Cheung W, Van Ness B. The bone marrow stromal microenvironment influences myeloma therapeutic response *in vitro*. Leukemia 2001;15: 264 – 71.

25. Shaughnessy JD. Amplification and overexpression of CKS1B at chromosome band 1q21 is associated with reduced levels of p27Kip1 and an aggressive clinical course in multiple myeloma. Hematology 2005;10: 117 – 26.

26. Sureau F, Moreau F, Millot JM, et al. Microspectrofluorometry of the protonation state of ellipticine, an antitumor alkaloid, in single cells. Biophys J 1993;65:1767 – 74.

27. Futscher BW, Blake LL, Gerlach JH, Grogan TM, Dalton WS. Quantitative polymerase chain-reaction analysis of MDR1 mRNA in multiple myeloma cell lines and clinical specimens. Anal Biochem 1993; 213:414 – 21.

28. Yanamandra N, Colaco N, Parquet N, et al Tipifarnib and bortezomib are synergistic and overcome cell adhesion-mediated drug resistance in multiple myeloma and acute myeloid leukemia. Clin Cancer Res 2006;12: 591 – 9.

29. Kuehl M, Bergsagel P. Multiple myeloma: evolving genetic events and host interactions. Nat Rev Cancer 2002;2:175 – 87.

30. Gottesman MM. Mechanisms of cancer drug resistance. Annu Rev Med 2002;53:615 – 27.

31. Jagannath S, Barlogie B, Berenson J, et al. A phase 2 study of two doses of bortezomib in relapsed or refractory myeloma. Br J Haematol 2004;27:165 – 72.